Thermal Analysis of the MRB during Downhill Braking

Hoang Quang Tuan [1], Vu Hai Quan [1], and Trinh Minh Hoang [2,*]

[1] School of Mechanical and Automotive Engineering, Hanoi University of Industry, Hanoi, Vietnam
[2] School of Mechanical Engineering, Hanoi University Science and Technology, Hanoi, Vietnam
Email: tuanhq@haui.edu.vn (H.Q.T.); quanvh@haui.edu.vn (V.H.Q.); hoang.trinhminh@hust.edu.vn (T.M.H.)
*Corresponding author

***Abstract*—This study focuses on simulating the heat generation in Magnetorheological Brakes (MRBs) during vehicle descent under standardized test conditions. The simulation results indicate that, under both test scenarios with slopes of 6% and 11%, the temperature generated in the MRB exceeds the permissible limits of the brake material. To address this issue, a cooling solution was implemented through thermal simulations using the numerical simulation software STAR-CCM+. Specifically, water jackets arranged around the brake casing and coils were used for cooling, resulting in an average temperature reduction of over 68% in both test scenarios. These findings highlight the potential for practical application of MRBs in actual vehicles by ensuring their thermal performance remains within safe operating limits.**

***keywords*—Magnetorheological Brakes (MRBs), Magnetorheological Fluid (MRF), thermal simulation, cooling solution**

I. INTRODUCTION

The braking process for trucks operating on steep and extended mountainous terrains has garnered significant attention from researchers [1–4]. In conventional braking systems, excessive temperature rise can result in brake failure, diminished braking efficiency, and heightened accident risks [5]. To mitigate these issues, trucks are equipped with auxiliary braking systems in addition to the primary braking system. These auxiliary systems help reduce the load on the main brakes, thereby improving safety and braking efficiency, particularly during downhill operations [6–7].

Among auxiliary braking technologies, systems utilizing smart materials, such as Magnetorheological Brakes (MRBs), have emerged as an innovative solution. MRBs offer effective brake force control and rapid response, enabled by the unique properties of Magnetorheological Fluids (MRF) [8–11]. However, the challenge of heat generation during MRB operation has been extensively investigated in numerous studies, as it remains a critical factor affecting the performance and durability of these systems [12–15].

Numerous studies have examined the impact of temperature on the performance of Magnetorheological Brakes (MRBs). Two methods for thermal analysis of MRBs installed on a ¼ car model were proposed in [16]. For automotive braking systems, the kinetic energy generated by the wheel's rotational motion is converted into thermal energy due to frictional stress. According to the law of energy conservation, the heat generated during braking (in Joules) equals the change in the vehicle's kinetic energy. Simulations revealed that the maximum steady-state temperature in the brake reached 365.3 K (92.3 °C), which is lower than the maximum operating temperature of MRF-132DG (130 °C).

Gang *et al.* [17] investigated the effect of key vehicle operating parameters on the maximum surface temperature of the brake disc. Results indicated that as the slope increased from 3° to 9°, the maximum brake disc temperature rose by 41.6%. In contrast, when the vehicle weight increased from 4 to 7 tons, the brake disc temperature showed a smaller increase of 16.7%. Chen *et al.* [18] conducted experimental studies to analyze the effect of high temperatures, particularly above 100 °C, on MR braking devices. Wang *et al.* [19] explored the transmission characteristics of MRBs under high braking torque. Their findings revealed that as the temperature increased from 25 °C to 150 °C, the braking torque initially increased but later decreased, with a reduction of approximately 210 Nm, from 1800 Nm to 1590 Nm.

Satyajit [20] presented a thermal analysis of MRBs for light two-wheeled vehicles, such as electric bicycles, under real-world urban conditions in India. The study aimed to estimate the temperature rise of the MR fluid during braking and to ensure it remained within the allowable operating range. Results confirmed that the MR fluid temperature consistently stayed within the permissible range (–40°C to 125 °C), demonstrating that the proposed MRB could operate safely without requiring specialized cooling mechanisms. Similarly, Thang [21] proposed a thermal analysis model for MRBs on motorcycles to replace conventional hydraulic disc brakes. This model enabled the evaluation of MR fluid temperature in both the active and inactive states of MRBs,

Manuscript received October 29, 2024; revised November 28, 2024; accepted December 26, 2024; published May 12, 2025.

doi: 10.18178/ijmerr.14.3.245-251

ensuring that the temperature always remained within the allowable limit. The model employed Navier-Stokes equations to simulate the flow of MR fluid within the brake and solved heat transfer equations to calculate the heat generated and dissipated into the surrounding environment.

While these studies provide valuable insights into the relationship between temperature and the performance of MRBs, they primarily focus on the behavior of MR fluids and do not comprehensively investigate the thermal performance of MRBs as auxiliary braking systems during prolonged downhill descents. Additionally, none of the studies have conducted simulations to analyze the cooling process for overheated MRBs, representing a gap in the current research. Building on this foundation, the present study aims to investigate the thermal behavior of magnetorheological brakes (MRBs) during vehicle descent and to propose effective cooling solutions to ensure efficient and safe operation under standardized downhill test conditions [6, 7].

II. Literature Review

The thermal behavior of Magnetorheological Brakes (MRBs) installed on vehicles is typically analyzed using two primary approaches [16, 19].

The first approach is grounded in the law of energy conservation, where the kinetic energy generated by the rotational velocity of the wheels is transformed into thermal energy through friction within the braking mechanism. The heat produced during braking is balanced by the change in the vehicle's kinetic or potential energy as it descends.

The second approach focuses on friction at the contact surfaces within the MRB. Frictional heat generated in the brake is partially absorbed by the rotor and the casing, while another portion is absorbed by the Magnetorheological Fluid (MRF). Under the influence of a magnetic field during braking, the MRF behaves as a solid. Consequently, in this method, thermal analysis is based on heat conduction between two solid bodies. Since MRBs do not experience wear during braking, the contact between MRF particles and the surrounding metal surfaces is considered ideal.

When analyzing heat transfer in MRBs during current-induced activation of the coil, two primary heat transfer mechanisms are typically considered:

- Conduction: Heat is conducted from the MRF to the rotor, and subsequently from the rotor to the casing.
- Convection: Heat is dissipated from the casing to the surrounding air via convective processes.

The investigation of the vehicle's downhill descent was conducted following the standard test procedure [6–7], utilizing both of the aforementioned approaches. In this scenario, it is assumed that the driver employs the MRB to maintain the vehicle's motion at a constant velocity v_2. Consequently, the force balance Eq. (1) is applied.

$$G\sin\alpha_0 = F_{p1} + F_{p2} + F_b + F_w + (F_{f1} + F_{f2}) + F_{ep} \quad (1)$$

where: F_w: Air resistance (N); F_{pi}: Braking force generated by the main braking system (N); F_b: Braking force generated by the auxiliary braking system (N); F_{fi}: Rolling resistance (N); α_0: Road slope angle (º); F_b - Braking force generated by the auxiliary braking system at the rear wheels; F_{ep}: Braking force generated by the engine at the rear wheels. The indices $i = 1, 2$ correspond to the forces and moments applied to the front and rear axles, respectively.

The effectiveness of auxiliary brakes under harsh operating conditions is evaluated in accordance with established standards [6, 7]. Specifically, for vehicles in categories M and N, the test requires maintaining a constant speed of $v_b = 30$ km/h over a distance of S = 6 km on a slope with a gradient of 6%, with the engine disconnected from the drivetrain (Fig. 1).

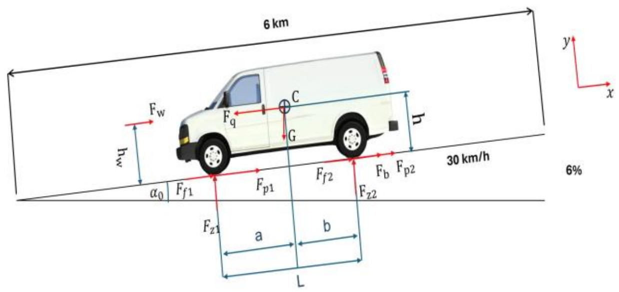

Fig. 1. Diagram of the vehicle braking system when descending a slope according to ISO 12161:2006.

Assuming downhill braking with the engine disconnected from the drivetrain, Eq. (1) can be rewritten as follows:

$$G\sin\alpha_0 = F_{p1} + F_{p2} + F_b + F_w + (F_{f1} + F_{f2}) \quad (2)$$

In accordance with the standard, during the auxiliary braking test for long downhill descents, the main braking system, engine braking, and additional systems such as the parking brake are not utilized. Furthermore, air resistance is neglected in the calculations and assumptions. Consequently, if longitudinal wheel slip is disregarded, the braking force generated by the auxiliary braking system (at the wheels) can be expressed as follows:

$$F_b = G\sin\alpha_0 - (F_{f1} + F_{f2}) = G\sin\alpha_0 - Gf\cos\alpha_0 \quad (3)$$

The braking torque required from the auxiliary braking system to maintain a constant vehicle speed (v_b) during a prolonged downhill descent is determined as follows:

$$T = F_b r_b / i_0 \quad (4)$$

The power required from the auxiliary braking system to sustain a constant vehicle speed during a prolonged downhill descent is expressed as:

$$P_{MRB} = T\omega_{MRB} \quad (5)$$

where:

$$\omega_{MRB} = \frac{v_b i_0}{r_b} \quad (6)$$

The heat energy dissipated by the auxiliary braking system to maintain a constant vehicle speed vbv_bvb over a prolonged downhill distance SSS is calculated as:

$$E_{MRB} = P_{MRB}\frac{S}{v_b} \tag{7}$$

III. Materials and Methods

The STAR-CCM+ software is employed to simulate the thermal behavior of the Magnetorheological Brake (MRB) by generating distinct physical models tailored for each component. These models account for the interaction between the Magnetorheological Fluid (MRF) and the magnetic field produced by the coil, as well as the movement of the surrounding air. Each model is designed to replicate real-world conditions, thereby enhancing the simulation's accuracy and effectiveness.

When simulating the thermal behavior of the MRB using STAR-CCM+, several critical assumptions are made to ensure the reliability of the results. It is assumed that the thermal and magnetic properties of the MRF and other system materials are homogeneous and remain constant over time. Parameters such as viscosity, thermal conductivity, and the thermal expansion coefficient of the MRF are predefined and remain unchanged during the simulation. The contact surfaces between brake components are assumed to be in perfect contact with no gaps. The flow of the MRF within the brake is considered laminar, and heat transfer in the system is modeled as occurring via conduction and convection, with no heat transfer through radiation.

Experiments under varying heat power conditions revealed that applying heat power directly to the MRF yielded the most favorable results. The simulation demonstrated that temperature increases over time and propagates to other components in the brake system. To simulate the heat dissipation environment, the vehicle's movement was modeled at a constant speed of v_b=30 km/h. Accordingly, the air inflow and outflow were set to correspond to this speed, with the inlet and outlet configurations depicted in Fig. 2.

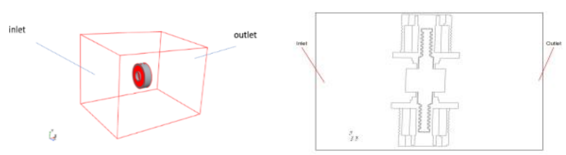

Fig. 2. Computational space.

To ensure computational accuracy, the grid was refined in regions with smaller dimensions, while coarser grids were applied to the outer air regions to minimize computational load. Grid sizes were optimized between 1 mm and 5 mm in different regions, tailored to meet the specific requirements of the analysis (Fig. 3).

Material: The brake material chosen is medium-carbon steel. The brake material and the MRF can be customized if sufficient material data are available (Fig. 4). Notably, it is assumed that the MRF does not degrade during operation. The thermal properties of AISI 1045 steel and MRF140CG magnetorheological fluid are obtained from the manufacturer's specifications and referenced in Table I.

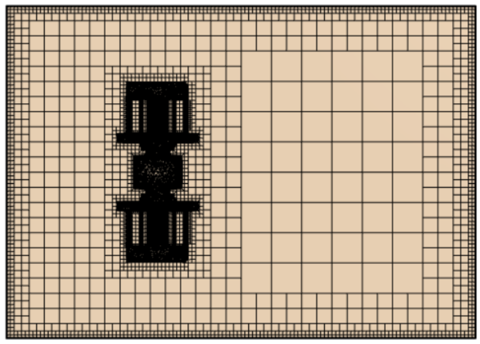
Fig. 3. Computational Grid Cross-section.

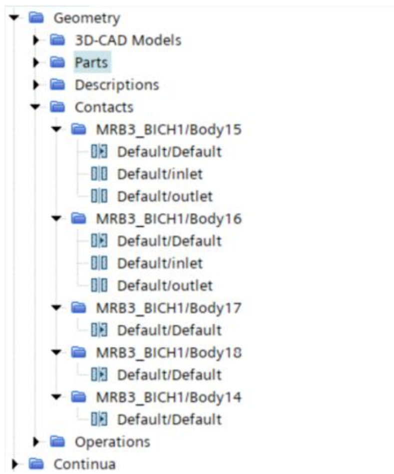

Fig. 4. Connections between elements.

TABLE I. Thermal Property Parameters for AISI 1045 Steel and MRF140CG

Thermal Properties	Items	Value
AISI 1045 Steel [22]	Specific Heat Capacity	0.49 J/g·°C or 490 J/kg·°C
	Thermal Conductivity	49.8 W/m·K (at 25 °C)
	Thermal Expansion Coefficient	11.2 µm/m·°C (in the range of 20 °C to 200 °C)
	Melting Point	1515°C (2760 °F)
	Temperature Resistance	Below 538 °C (1000 °F)
	Optimal working temperature	–29°C to 400°C
MRF140CG [23]	Maximum operating temperature	130 °C
	Freezing point temperature	–40 °C

Thermal connections were established between the various components to ensure efficient heat transfer. These include connections between the brake and the fluid, the brake and the coil, and the brake and the surrounding air.

IV. Result and Discussion

In this study, the energy (expressed as power P_{MRB}) and current I_{MRB} of the auxiliary braking system are evaluated within the operational range of the MRB, which includes road slopes from 6% to 11%, and vehicle speeds on downhill roads ranging from 20 km/h to 40 km/h [7]. Based on the structural parameters of the wheel radius r_b = 0.284 m and the final drive ratio i_0 = 5.125 [24], the operational rotational speed of the MRB, calculated using Eq. (6), is determined to range from 1436.7 rpm to 2393.4 rpm, as summarized in Table II.

TABLE II. CALCULATION OF WHEEL SPEED CONVERSION TO MRB ROTATIONAL SPEED

V_b(km/h)	$\omega_b = V_b/(3.6\times r_b)$ (rad/s)	$\omega_{MRB} = \omega_b/io$ (rad/s)	n_{MRB} (rpm)
50	48.90	250.63	2393.4
40	39.12	200.50	1915.6
30	29.34	150.38	1436.7

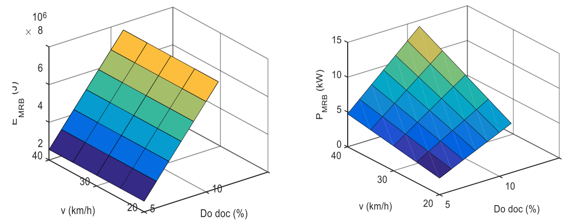

Fig. 5. Energy (E_{MRB}) and Power (P_{MRB}) of the MRB to maintain vehicle speed on a slope.

Fig. 5 and Table III illustrates the energy and thermal power required by the MRB to maintain the vehicle at various steady speeds (ranging from 20 km/h to 50 km/h) while descending a slope with a constant gradient (ranging from 5% to 11%) over a downhill distance of S = 6 km, in accordance with ISO testing standards.

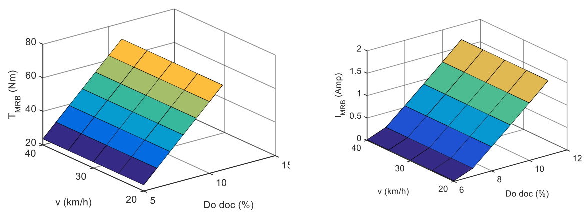

Fig. 6. Torque and current of the MRB to maintain vehicle speed on a slope.

Fig. 6 illustrates the torque generated by the MRB and the corresponding current required by the auxiliary braking system under each test condition. In the standard test mode (vehicle descending at a speed of v_b = 30 km/h on a slope of 6%), the thermal energy dissipated by the MRB is 6.81×106 J (equivalent to a power of 4.73 kW), Under these conditions, the MRB generates a torque of 31.47 Nm, requiring a current supply of 0.0 A (see Table I). In the maximum test condition (v_b = 40 km/h on a slope of 11%), the MRB dissipates thermal energy amounting to 11.03×106 J (equivalent to a power of 14.14 kW). At this point, the MRB generates a torque of 70.52 Nm, corresponding to a current supply of 1.7 A. These results serve as the foundational input for the thermal analysis of the MRB.

TABLE III. CALCULATION OF THE POWER REQUIRED BY THE MRB TO MAINTAIN THE VEHICLE AT VARIOUS STEADY SPEEDS (WITHIN THE RANGE OF 20 KM/H TO 50 KM/H) WHILE TRAVELING ON A SLOPE WITH A SONSTANT INCLINE (WITHIN THE RANGE OF 5% TO 11%) OVER A DOWNHILL DISTANCE OF S = 6 KM ACCORDING TO ISO TESTING STANDARDS

Speed v_b	slope (%)						
(km/h)	5	6	7	8	9	10	11
20	2.37	3.16	3.94	4.73	5.51	6.29	7.07
25	2.96	3.94	4.93	5.91	6.89	7.86	8.84
30	3.55	4.73	5.91	7.09	8.26	9.44	10.60
35	4.14	5.52	6.90	8.27	9.64	11.01	12.37
40	4.74	6.31	7.88	9.45	11.02	12.58	14.14

A. Thermal Analysis of the MRB without Cooling

1) Thermal analysis of the MRB in standard testing mode

The thermal analysis of the MRB is performed under standard testing conditions, where the vehicle descends at a speed of v_b = 30 km/h on a road incline of 6%. Under these conditions, the thermal simulation indicates that the MRB must dissipate thermal energy amounting to 6.81×10^6 J (equivalent to a power of 4.73 kW), with a current supply to the MRB of 0.9 A.

The temperature field analysis of the MRB disc brake, illustrated in Fig. 7, reveals that the highest temperature is concentrated at the contact area between the brake disc and the MR fluid layer. The temperature gradually decreases with increasing distance from this contact area, reaching its lowest point at the outer edge of the brake disc relative to the axis of rotation. The temperature distribution across the MRB is notably uneven, with the MR fluid region and the brake disc identified as the hottest areas.

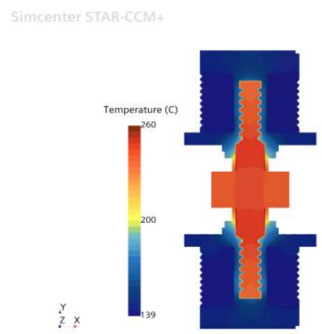

Fig. 7. Temperature distribution in the brake cross-section for the case of 7 teeth without cooling.

This phenomenon occurs because the contact area between the MR fluid and the brake disc is the primary site of friction during braking, resulting in significant heat generation. This thermal energy is transferred from the MR Fluid (MRF) to the brake disc and subsequently to the brake casing. The heat is then dissipated into the surrounding environment through fundamental heat transfer mechanisms, including conduction and radiation.

The results presented in Fig. 8 indicate that the temperatures of the primary components of the 7-tooth MRB brake exhibit a linear increase, reaching approximately 261 °C. The highest temperature, approximately 261.6 °C, is observed at the rotor, while the coil reaches a maximum temperature of approximately 226 °C during the 12-minute (720-second) observation period. The brake housing, being the coolest component, achieves a maximum temperature of 223.8 °C at the end of the analysis.

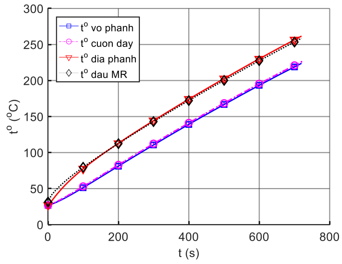

Fig. 8. Temperatures of the main components of the MRB at a slope of 6%.

As shown in Fig. 9, the highest air velocity occurs in the region directly in front of the brake, gradually decreasing as it passes through the brake and approaching nearly zero in the area behind the brake. The airflow direction is from left to right. Upon encountering the brake, the airflow splits into two branches, which subsequently merge again after passing the brake.

The MRB's structure creates an obstruction to the airflow, reducing air velocity and contributing to the cooling process. Due to the disc-shaped design of the MRB with serrated fins, drag is generated, further decreasing airflow velocity while increasing the contact area between the air and the brake. This configuration enhances the dissipation of heat from the brake to the surrounding environment, improving its thermal performance.

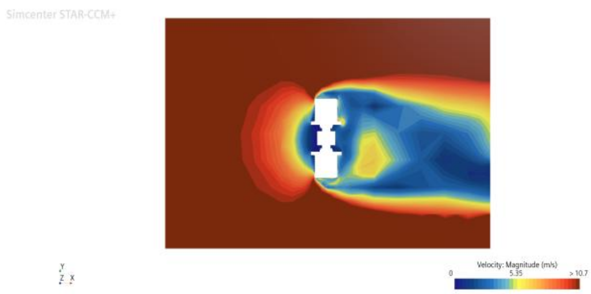

Fig. 9. Air velocity field in the environment.

2) Thermal analysis of the MRB under maximum slope testing conditions

In a manner similar to the 6% slope scenario, this study simulates the thermal energy generated when maintaining a vehicle speed of v_b =30 km/h on an incline with a maximum slope of 11%. The thermal energy in this case amounts to 7.66×10^6 J (equivalent to a power of 14.1 kW). Under these conditions, the MRB must generate a torque of 70.7 Nm, corresponding to a current supply of 1.7 A. The temperature results for the primary components of the MRB under these testing conditions are illustrated in Fig. 10. The findings reveal a continuous increase in temperature, with the main components of the 7-tooth MRB brake reaching temperatures exceeding 72 °C after 12 min of testing. The highest temperature is recorded at the rotor, reaching 722.6 °C at the 12th minute, while the lowest temperature is observed at the brake housing, at 607.3 °C at the same time point.. The thermal analysis results under both standard testing conditions and maximum slope conditions on Vietnamese roads indicate that the temperatures within the MRB exceed the operational temperature limit of the magnetorheological fluid [23, 25]. These findings highlight the critical need to implement an effective cooling strategy for the MRB to ensure its safe and efficient operation.

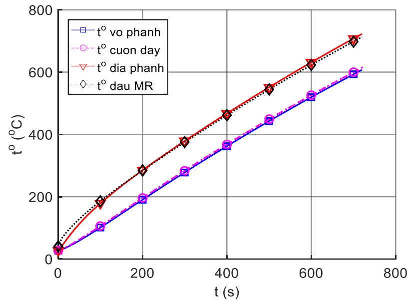

Fig. 10. Temperature of the main components of the MRB in the testing mode with an 11% incline.

B. Thermal Analysis of the MRB with a Cooling Strategy

There are various cooling methods available, including natural air cooling, water cooling, oil cooling, and cooling using materials with high thermal conductivity. The selection of an appropriate cooling method depends on several factors, such as the operating temperature requirements of the MRB, operating conditions (e.g., heavy loads, high-temperature environments), and specific applications (e.g., automotive, industrial, aerospace) [26, 27].

In this paper, the authors selected the water jacket cooling method. Based on the original structure of the MRB (Fig. 11(a)), this cooling strategy involves arranging water jackets around the coil area, where it interfaces with the brake casing (Fig. 11(b)). This method was chosen for its numerous advantages, including high cooling efficiency, maintaining stable temperatures, the ability to cool localized hot spots, suitability for high-power applications, and reducing the size and weight of the cooling system.

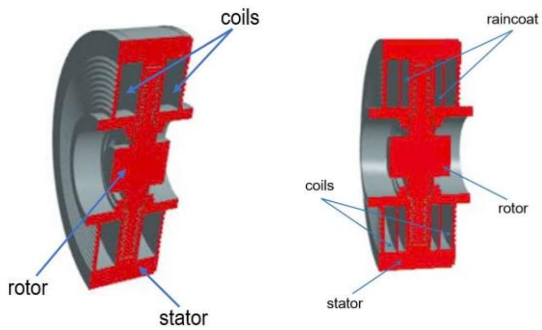

(a) (b)

Fig. 11. Cross-section of the 7-tooth brake (a) without water jackets; (b) with water jackets.

1) Thermal analysis of the MRB under standard testing conditions (with cooling)

Fig. 12 illustrates the velocity distribution of the cooling water flow within the MRB brake. The results show that the highest water flow velocity is observed near the inlet (right side) and outlet of the water channel, gradually decreasing as the flow moves deeper into the channel, with the lowest velocity occurring near the surface of the MRB. The cooling water enters through the inlet, passes through the water channel, and exits through the outlet, which has the smallest cross-sectional area.

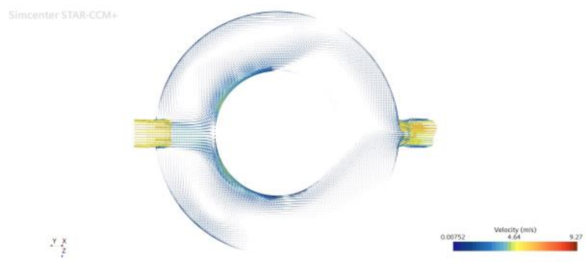

Fig. 12. Velocity vector of the cooling water flow.

According to Bernoulli's principle, the flow velocity increases as the cross-sectional area decreases. Additionally, a swirling flow pattern is observed near the surface of the MRB. The cooling water flows through the water jacket with an uneven velocity distribution, with the highest velocities concentrated near the inlet and outlet regions of the channel. This swirling flow pattern enhances the cooling efficiency of the MRB by increasing the heat transfer rate between the cooling water and the brake surface.

The analysis of the temperature distribution across the cross-section of the disc-type MRB brake exhibits a similar pattern to that observed in the non-cooled scenario. However, the average temperature profile of the MRB brake, as shown in Fig. 13, reveals distinct phases of temperature change. Initially, the temperatures of the various components rise rapidly, followed by a slower increase, eventually stabilizing after approximately 12 min (720 s).

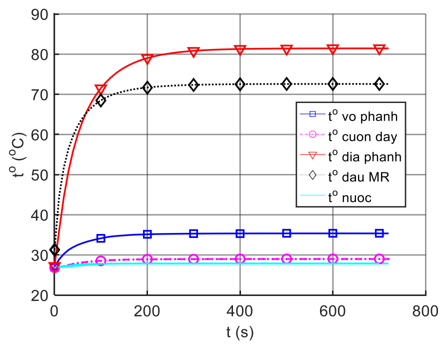

Fig. 13. Temperature of the main components of the MRB at a 6% slope (with cooling).

During the first 200 s, the average temperature of the brake shows a gradual increase. Subsequently, the primary components of the brake, including the brake disc and the Magnetorheological Fluid (MRF), reach a stable temperature of approximately 80 °C after 12 min of continuous operation. This temperature stabilization is attributed to the effective and continuous cooling provided to the stator and the coil.

The results of the average thermal simulation of the MRB under maximum slope testing conditions (11%) with the implemented cooling scheme are presented in Fig. 14. In the cooled scenario, the temperature of the brake disc decreased significantly, stabilizing at levels below 192 °C. The simulation results for the maximum slope of 11% further indicate that the temperatures of the cooling water, coil, and brake casing remained stable, all below 50 °C.

However, the temperature of the Magnetorheological Fluid (MRF) exceeded the manufacturer's recommended operating range (below 165°C). This finding highlights the necessity of employing more effective cooling measures in the design of MRBs intended for operation on steep gradients. Furthermore, careful consideration should be given to the arrangement of the water jackets to ensure continuous water circulation in the stator region of the brake while addressing spatial constraints in the design process.

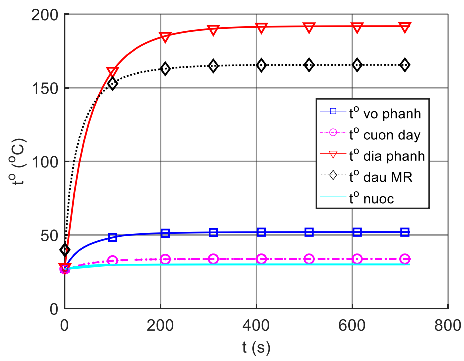

Fig. 14. Temperature of the main components of the MRB in the testing mode with an 11% slope (with cooling).

V. Conclusion

This study developed a theoretical model to investigate the braking process during vehicle descent on slopes, adhering to auxiliary brake standards. The model serves as the foundation for analyzing thermal behavior based on the law of energy conservation and heat transfer principles. Using numerical simulation methods, the study revealed that the heat generated in the auxiliary brakes exceeds the permissible working limits of the materials.

To address this issue, a water cooling solution was simulated to enhance the performance of the MRB when installed on a vehicle. In the test conducted on a standard slope (6%), the cooling solution achieved a temperature reduction of over 68.6% for the main components of the MRB compared to the non-cooled scenario, with the highest cooling efficiency observed in the brake casing. Similarly, in the test conducted on a maximum slope (11%) with a vehicle speed maintained at 40 km/h, the cooling solution achieved a temperature reduction of over 73.4% for the main components of the MRB compared to the non-cooled condition.

These results clearly demonstrate the effectiveness of the water cooling solution when the vehicle descends steep slopes. The highest cooling efficiency was observed in the brake casing, which benefits from direct contact with ambient air and the internal arrangement of water jackets within the MRB. The findings of this study provide valuable insights and important directions for the practical development and implementation of MRBs in vehicle applications.

This paper presents a method for simulating the heat generated under different operating conditions of MRB. The research results provide a foundation for designing and applying MRBs on actual vehicles. Additionally, experimental validation will be conducted on a test bench that the authors have directly designed and fabricated.

The test bench is fundamentally capable of replicating conditions such as brake disc rotational speeds, coil current intensities, and experimental durations corresponding to the simulations. By installing temperature sensors at various positions on the MRB, it will be possible to measure the temperature rise of the MRB, thereby activating the cooling system when the MRB overheats. The results will be further published by the authors in the near future.

Conflict of Interest

The authors declare no conflict of interest

Author Contributions

Hoang Quang Tuan: Data curation, Conceptualization, Formal analysis, Software, Methodology, Writing—original draft, Writing—review & editing. Trinh Minh Hoang: Conceptualization, Formal analysis, Software, Methodology. Vu Hai Quan: Formal analysis, Writing—original draft, Writing—review & editing. All authors had approved the final version.

References

[1] M. Droege, "Heavy-duty truck platooning on hilly terrain: Methods for assessment and improvement," MS thesis, Purdue University, 2021.

[2] L. Jiaxin and Z. Jing, "Safety adaptability of engine retarder (Jacobs) on long downhill of expressways," *Journal of Physics: Conference Series*, IOP Publishing, vol. 1187, no. 3, 032105, 2019.

[3] Use of auxiliary brakes in heavy vehicles. (2014). Research Report AP-R456-14. [Online]. Available: https://austroads.gov.au/publications/freight/ap-r456-14

[4] Heavy vehicle brake safety on long and very steep roads. (2010). APR362/10. [Online]. Available: https://austroads.gov.au/publications/freight/ap-r362-10.

[5] Y. Xu, B. Mei, L. Xiao, X. Wanyang, and G. Tan, "Combined hill descent braking strategy for heavy truck in the featured-slope," *SAE Technical Paper*, pp. 0148–7191, 2017.

[6] ECRR13:2023. (2023). [Online]. Available: https://unece.org/sites/default/files/2024-03/R013r9e.pdf

[7] ISO12161:2006. (2006). [Online]. Available: https://www.iso.org/obp/ui/en/#iso:std:iso:12161:ed-1:v1:en

[8] L. K. George, N. Tamilarasan, and S. Thirumalini, "Design and analysis of magneto rheological fluid brake for an all terrain vehicle," *IOP Conference Series: Materials Science and Engineering*, IOP Publishing, vol. 310, no. 1, 012127, 2018.

[9] K. Karakoc, E. J. Park, and A. Suleman, "Design considerations for an automotive magnetorheological brake," *Mechatronics*, vol. 18, no. 8, pp. 434–447, 2008.

[10] H. Shamieh and R. Sedaghati, "Development, optimization, and control of a novel magnetorheological brake with no zero-field viscous torque for automotive applications," *Journal of Intelligent Material Systems and Structures*, vol. 29, no. 16, pp. 3199–3213, 2018.

[11] S. Xiong, G. Tan, B. Yang, L. Xiao, Y. Xu, and Y. Wang, "Effect of temperature on braking efficiency stability of magnetorheological fluid auxiliary braking devices," *SAE Technical Paper*, pp. 0148–7191, 2017.

[12] S. R. Patil, K. P. Powar, and S. M. Sawant, "Thermal analysis of magnetorheological brake for automotive application," *Applied Thermal Engineering*, vol. 98, pp. 238–245, 2016.

[13] W. Song, S. Wang, S.-B. Choi, N. Wang, and S. Xiu, "Thermal and tribological characteristics of a disc-type magnetorheological brake operated by the shear mode," *Journal of Intelligent Material Systems and Structures*, vol. 30, no. 5, pp. 722–733, 2019.

[14] W. Szelag, C. Jedryczka, A. Myszkowski, and R. M. Wojciechowski, "Coupled field analysis of phenomena in hybrid excited magnetorheological fluid brake," *Sensors*, vol. 23, no. 1, 358, 2022.

[15] J. Zhang, G. Hu, Q. Cheng, L. Yu, and W. Zhu, "Analysis of braking performance and heat dissipation characteristics of multi-disc magnetorheological brake with an inner water-cooling mechanism," *Journal of Magnetism and Magnetic Materials*, vol. 604, 172313, 2024.

[16] H. Shamieh, "Modelling, design optimization and control of magneto rheological brakes for automotive applications," Masters thesis, Concordia University, 2017.

[17] W. Gang, C. Tian, and L. ZhiPeng, "Study on the influence of running parameters on the temperature field of disc brake on long downhill road," in *Proc. the Institution of Mechanical Engineers, Part D: Journal of Automobile Engineering*, 2024, vol. 238, no. 10–11, pp. 3386–3398.

[18] S. Chen, J. Huang, K. Jian, and J. Ding, "Analysis of influence of temperature on magnetorheological fluid and transmission performance," *Advances in Materials Science and Engineering*, vol. 2015, pp. 1–7, 2015, doi: 10.1155/2015/583076

[19] D. Wang, B. Zi, Y. Zeng, F. Xie, and Y. Hou, "An investigation of thermal characteristics of a liquid-cooled magnetorheological fluid-based clutch," *Smart Materials and Structures*, vol. 24, no. 5, 2015. doi: 10.1088/0964-1726/24/5/055020

[20] S. R. Patila, K. P. Powarb, S. M. Sawanta, "Thermal analysis of magnetorheological brake for automotive application," *Applied Thermal Engineering*, vol. 98, pp. 238–245, 2016. doi: 10.1016/j.applthermaleng.2015.11.128

[21] T. Le-Duc *et al.*, "Multi-objective optimal design of magnetorheological brakes for motorcycling application considering thermal effect in working process," *Smart Mater. Struct.*, 2018. doi 10.1088/1361-665X/aacb40

[22] AISI 1045 Steel, cold drawn, high temperature stress relieved, 50-75 mm (2–3 in) round [Online]. Available: https://www.matweb.com/search/datasheet_print.aspx?matguid=193434cf42e343fab880e1dabdb143ba

[23] Magneto-Rheological Fluid. [Online]. Available: https://www.shoplordmr.com/mr-products/mrf-140cg-magneto-rheological-fluid-250ml

[24] H. Q. Tuan *et al.*, "Evaluation of the braking performance of van trucks when descending hills using auxiliary brakes," *Science-Technology*, 2023. doi: https://doi.org/10.57001/huih5804.2023.224

[25] H. Q.Tuan *et al.*, "A study the effect of key parameters on the magneto-rheological brake torque based on the simulation method", *ARPN Journal of Engineering and Applied Sciences*, 2023. https://doi.org/10.59018/0723192

[26] W. Song, W. Wang, and X. Jin, "Thermal analysis and cooling optimization of the magnetorheological brake," *Advanced Material Science and Engineering Amse 2016*, *World Scientific*, pp. 482–490, 2016. https://doi.org/10.1142/9789813141612_0066

[27] D. M. Wang, Y. F. Hou, and Z. Z. Tian, "A novel high-torque magnetorheological brake with a water cooling method for heat dissipation," *Smart Mater. Struct.*, vol. 22, 025019, 2013. doi: 10.1088/0964-1726/22/2/025019